

Supporting Information

A continuous fabrication of mechanochromic fiber

Jing Zhang, Sisi He, Lianmei Liu, Guozhen Guan, Xin Lu, Xuemei Sun, and
Huisheng Peng**

*State Key Laboratory of Molecular Engineering of Polymers, Collaborative
Innovation Center of Polymers and Polymer Composite Materials, Department of
Macromolecular Science, and Laboratory of Advanced Materials, Fudan University,
Shanghai 200438, China; E-mail: sunxm@fudan.edu.cn, penghs@fudan.edu.cn.*

Experimental Section

Materials. Sodium bisulfite (SBS) and sodium peroxodisulfate (SPS) were obtained from Sigma Aldrich. Potassium hydroxide (KOH) and sodium hydroxide (NaOH) were purchased from Sinopharm Chemical reagent Co., Ltd. Styrene, butanediol diacrylate (BDDA), sodium dodecylsulfate (SDS), allyl methacrylate (ALMA), methyl methacrylate (MMA), ethyl acrylate (EA) and inhibitor removal resin were purchased from Alfa Aesar. Prior to use in the reaction, styrene was purified by distilling under reduced pressure. BDDA and ALMA were destabilized by an inhibitor removal resin. EA was purified by washing with 1 mol/L NaOH aqueous solution for three times and washing with water until the solution was neutral, followed by drying with anhydrous sodium sulfate. For use in the reaction, deionized water was bubbled with argon for at least 30 min.

Synthesis of PS/PMMA/PEA core-shell microspheres. The core-shell microspheres were synthesized by semi-continuous and stepwise emulsion polymerization. In a typical synthesis, a mixture of 0.09 g of SDS, 1.8 g of styrene, 0.20 g of BDDA, and 108.5 g of deionized water was added to a 500 mL flask which was equipped with stirrer and reflux condenser. At an argon atmosphere, the system was heated to 75 °C under vigorous stirring (300 r/min). Then the polymerization was initiated by adding an aqueous solution of 25 mg of SBS, 175 mg of sodium SPS, and 25 mg of SBS in order. An increasing opalescence of mixture was observed within several minutes after adding the above-mentioned aqueous solution. After 30 min, a mixture of 3.3 g of BDDA, 29.7 g of S, 150 mg of SDS, 50 mg of KOH, and 45 g of deionized water was added continuously to the reaction system within 150 min. After another 30 min, 50 mg of SPS aqueous solution was added. After an additional 30 min, a mixture of 1.5 g of ALMA, 13.5 g of MMA, 75 mg of SDS, and 20 g of deionized water was added continuously into the reaction system within 45 min. After 30 min, a mixture of 65.0 g of EA, 165 mg of SDS, and 69.5 g of deionized water was added continuously to the reaction system within 240 min. The microspheres with different diameters were synthesized by varying the amount of SDS.

Continuous fabrication of mechanochromic fiber. The core-shell microsphere dispersions were concentrated by a rotary evaporation. The resulting solutions exhibited high solid contents of 38-50% (Table S1), and they were viscous (~2500

mPa·s) but stable. The hydrophilicity of black spandex fibers was enhanced by an oxygen plasma treatment at 900 W for 3 min. A mechanochromic fiber was continuously prepared by coating the concentrated microsphere dispersion onto the treated black spandex fiber with the assistance of two electric motors. First, the oxygen plasma-treated fiber was twisted around a wheel with a diameter of 7 cm with the end being fastened to another wheel which was fixed at an electric motor. The middle of the fiber hung in the air was then immersed in the concentrated microsphere dispersion in an open container. Next, the wheel driven by the electric motor was rotated to make the fiber immerse into the dispersion, and the resulting fiber was collected by the second electric motor. The two electric motors were rotated with the same linear speed of 1.32 m/min. Finally, the composite fiber was dried by an infrared heat lamp.

Preparation of mechanochromic materials based on the other substrates. The other mechanochromic materials were obtained by dip-coating the concentrated dispersion onto the different substrates. The thin structural colored film was fabricated by coating the concentrated dispersion onto a glass and then tearing off after drying.

Characterization. Photographs were taken using a digital camera (Nikon J1, Tokyo, Japan). Scanning electron microscopy (SEM) images were recorded using a field-emission scanning electron microscopy (Ultra 55, Zeiss), operated at 0.50 kV. The morphologies of microspheres were observed by transmission electron microscopy (TEM) (JEOL JEM-2100 F, Japan). The diameters and particle dispersion indices (PDI) of microspheres were characterized by dynamic light scattering (DLS) (Zetasizer Nano, Malvern). The viscosity data were obtained using Rotary Rheometer (HAAKE MARS III, Thermofisher). The black spandex fibers were treated through the oxygen microwave plasma at a pressure of 0.1 mbar and flow rate of oxygen gas of 300 sccm (Plasma System 690, PVA Tepla). The stress and strain in the stretching and releasing cycles were measured from a Hengyi Table-Top universal testing instrument. Reflection spectra were obtained using a miniature fiber optic spectrometer (Idealoitics PG2000-pro, China) installed in an optical microscopy (Olympus BX51, Japan). During the spectra acquisition process, the incident and reflected light was parallel and in the radial direction of the mechanochromic fiber (MCF).

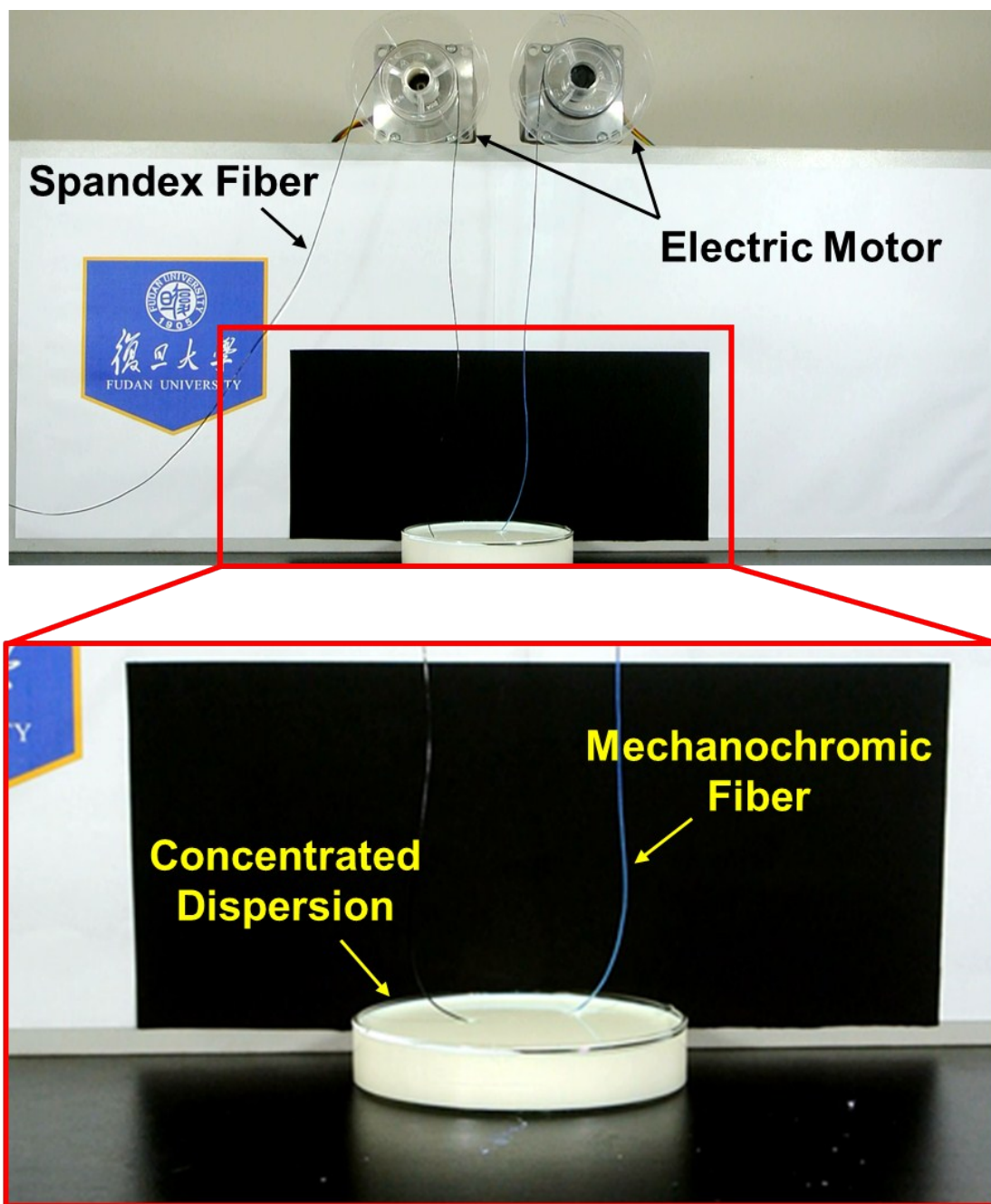


Figure S1. Photograph of the continuous preparation of MCFs.

Table S1. The diameter, PDI and diameter ratio of PS/PMMA/PEA core-shell microspheres and the solid content of microsphere dispersion.

	Color	Blue	Green	Red
Diameter	PS	143 nm	184 nm	202 nm
	PS/PMMA	164 nm	206 nm	240 nm
	PS/PMMA/PEA	216 nm	273 nm	324 nm
PDI	PS	0.019	0.027	0.036
	PS/PMMA	0.039	0.007	0.036
	PS/PMMA/PEA	0.011	0.017	0.009
Diameter ratio	PS/PMMA core	75.9%	75.5%	74.1%
	PEA shell	24.1%	24.5%	25.9%
Solid content	Original dispersion	35.9%	31.0%	25.4%
	Concentrated dispersion	50.4%	46.4%	38.1%

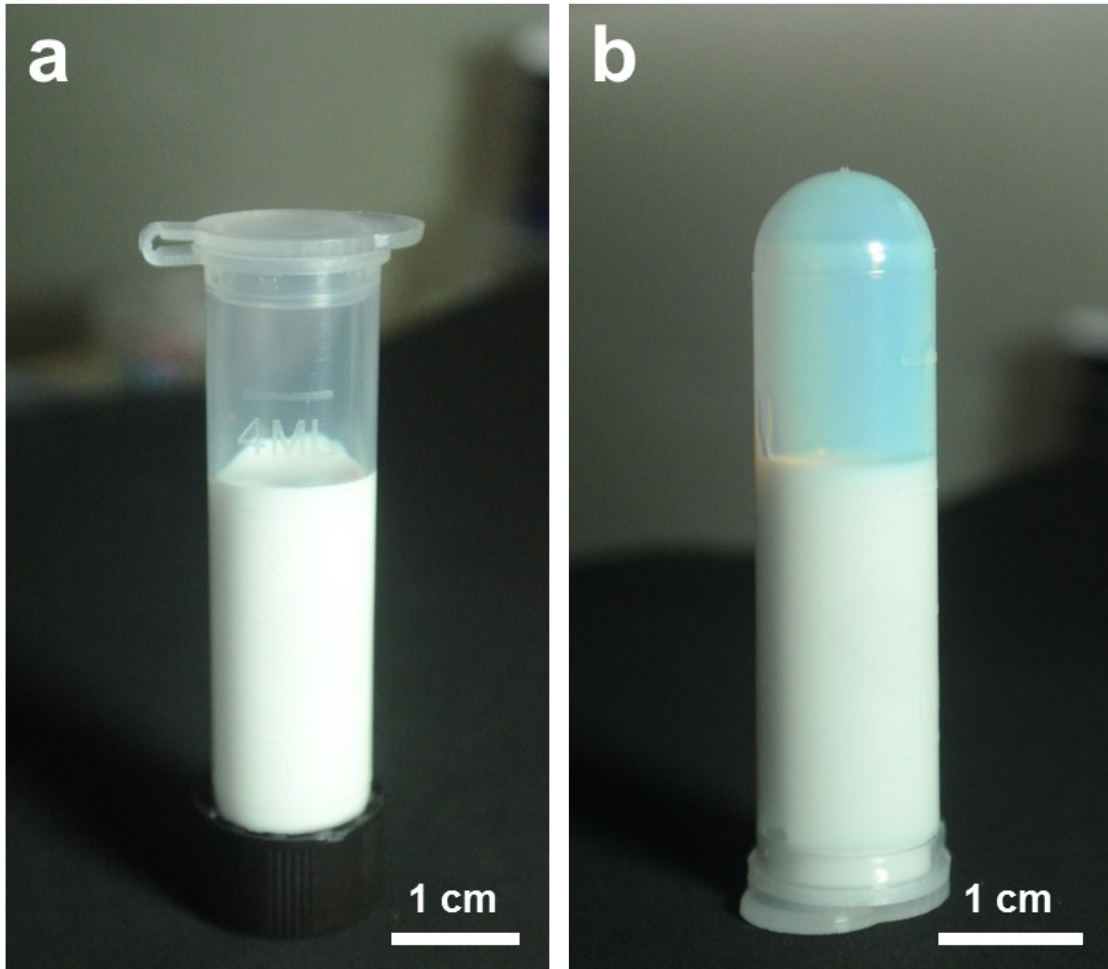


Figure S2. Photographs of the concentrated PS/PMMA/PEA core-shell microsphere dispersion that had been stored for 4 months.

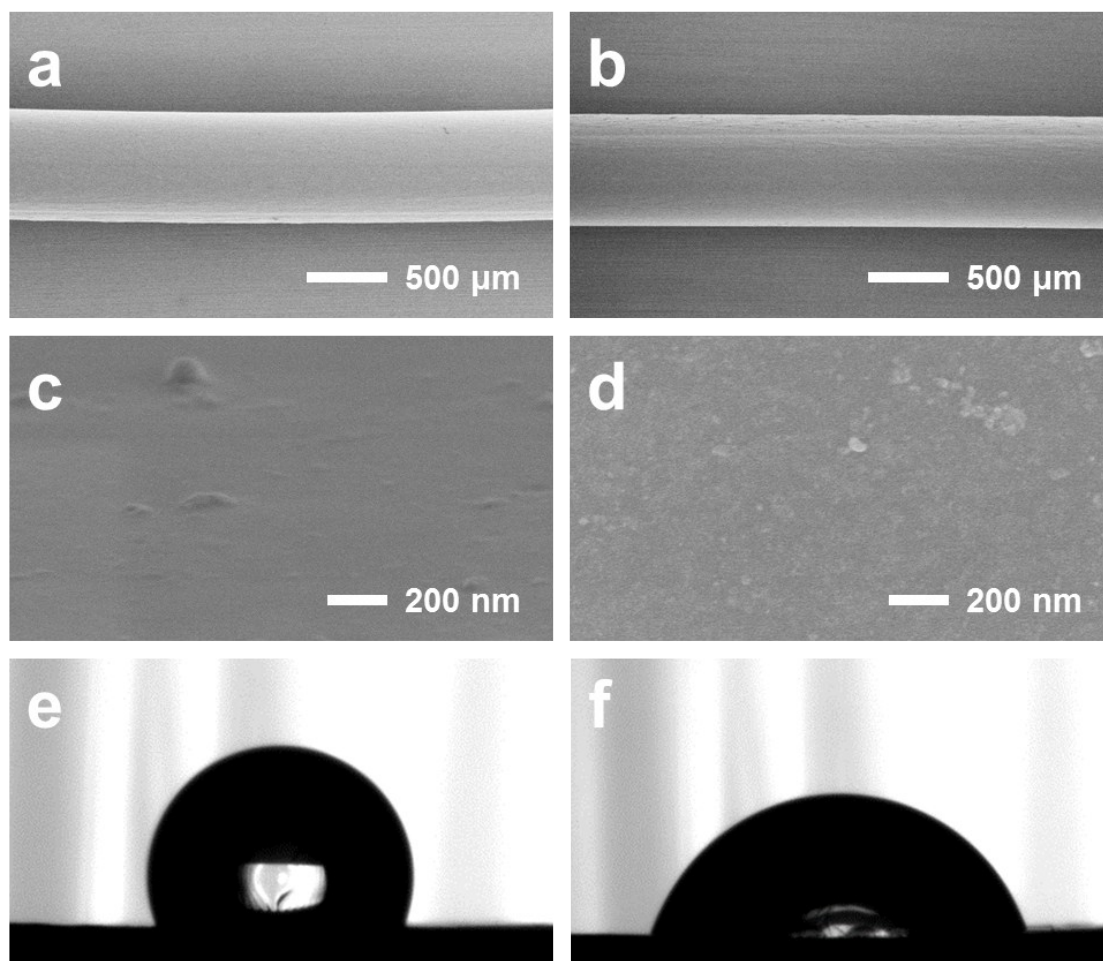


Figure S3. (a) SEM image of black spandex fiber. (b) SEM image of oxygen plasma-treated black spandex fiber. (c) SEM image of (a) at a higher magnification. (d) SEM image of (b) at a higher magnification. (e) and (f) The water contact angle of spandex fiber before (e) and after (f) oxygen plasma treatment.

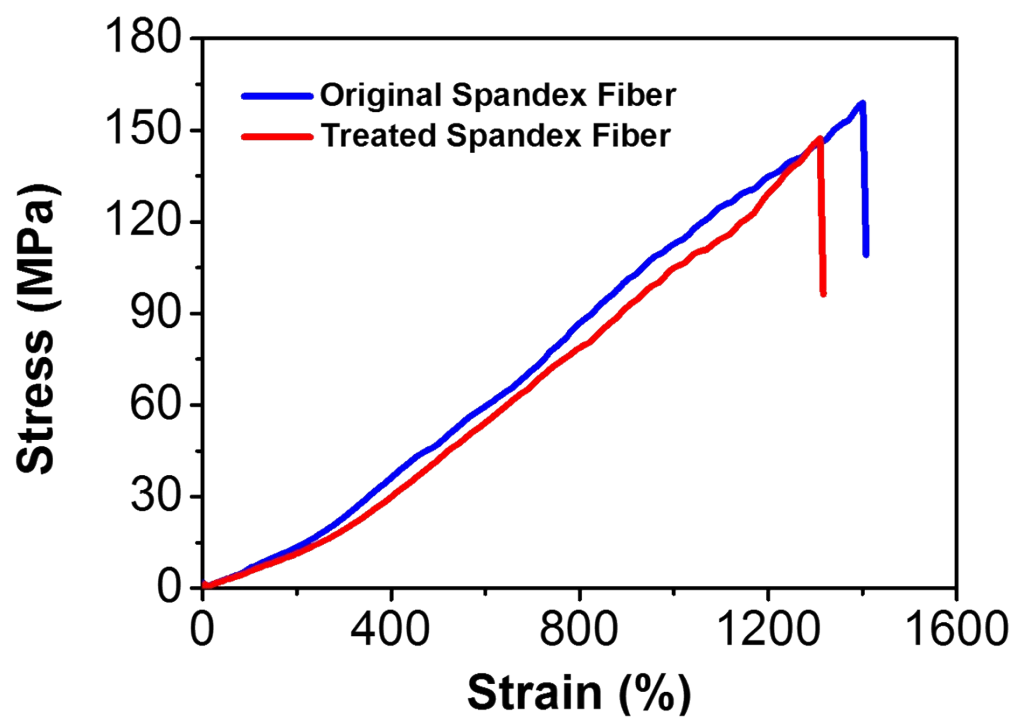


Figure S4. Stress-strain curves of the spandex fibers before and after oxygen plasma treatment.

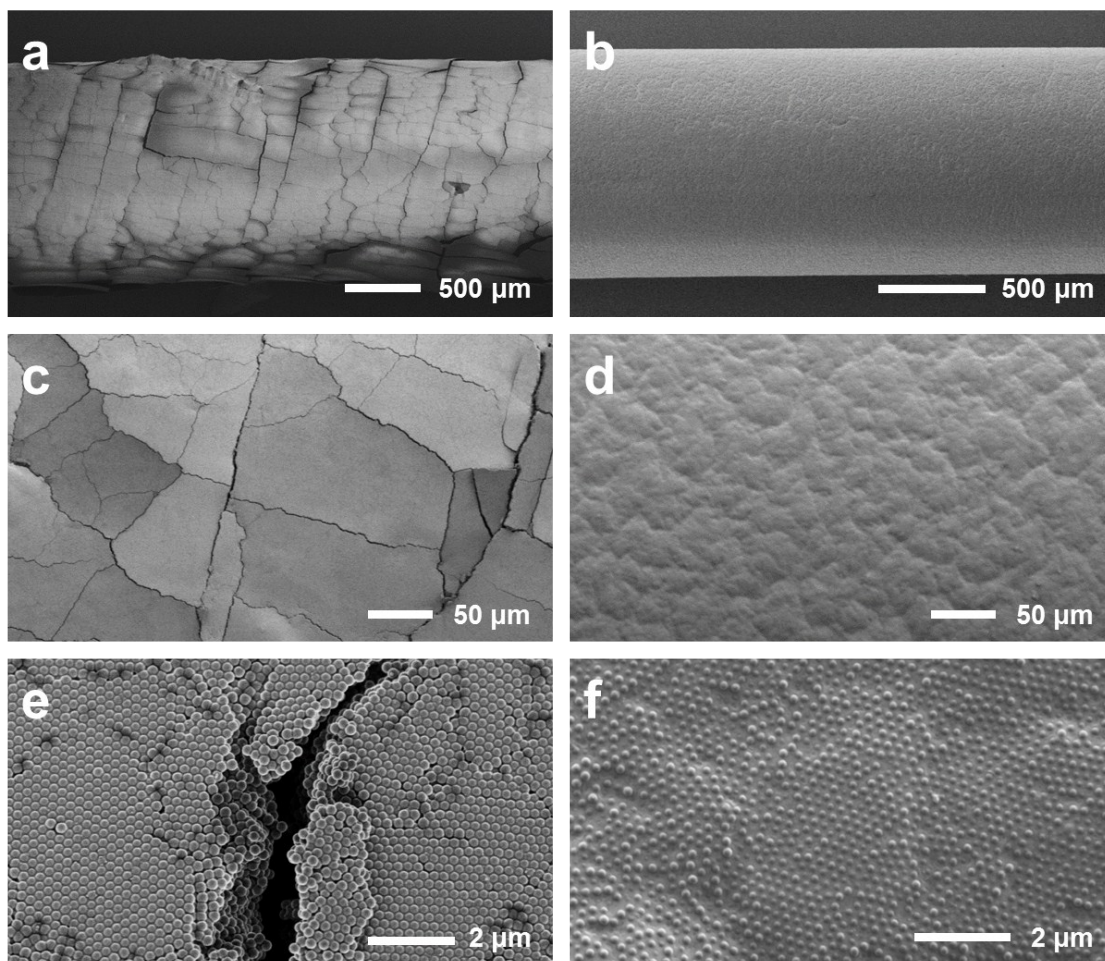


Figure S5. (a) and (b) SEM images of MCFs from PS microspheres with a diameter of 240 nm and PS/PMMA/PEA core-shell microspheres, respectively. (c) and (e) Higher magnification of (a). (d) and (f) Higher magnification of (b).

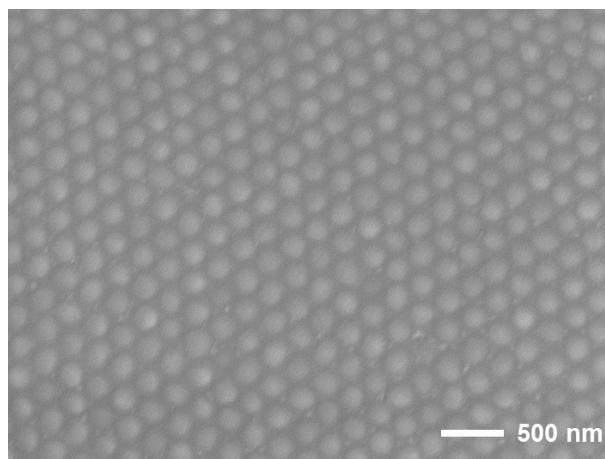


Figure S6. SEM image of PS/PMMA/PEA core-shell microspheres on a planar glass substrate.

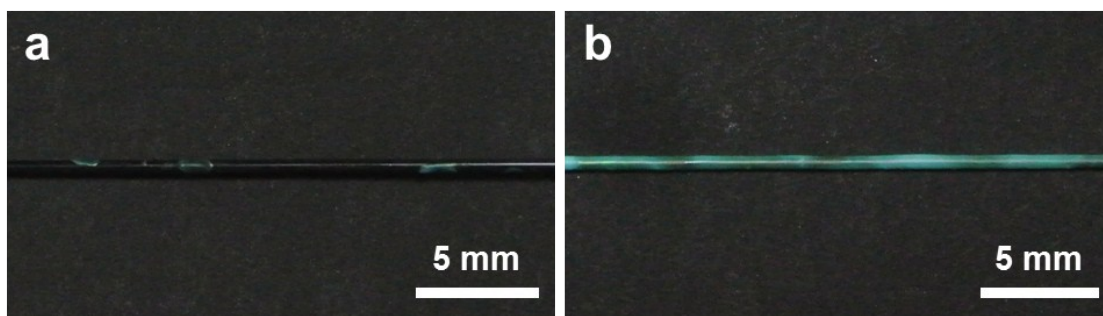


Figure S7. (a) Photograph of a MCF based on the microsphere dispersion with a lower solid content of ~31 %. (b) Photograph of a MCF based on the spandex fiber without plasma treatment.

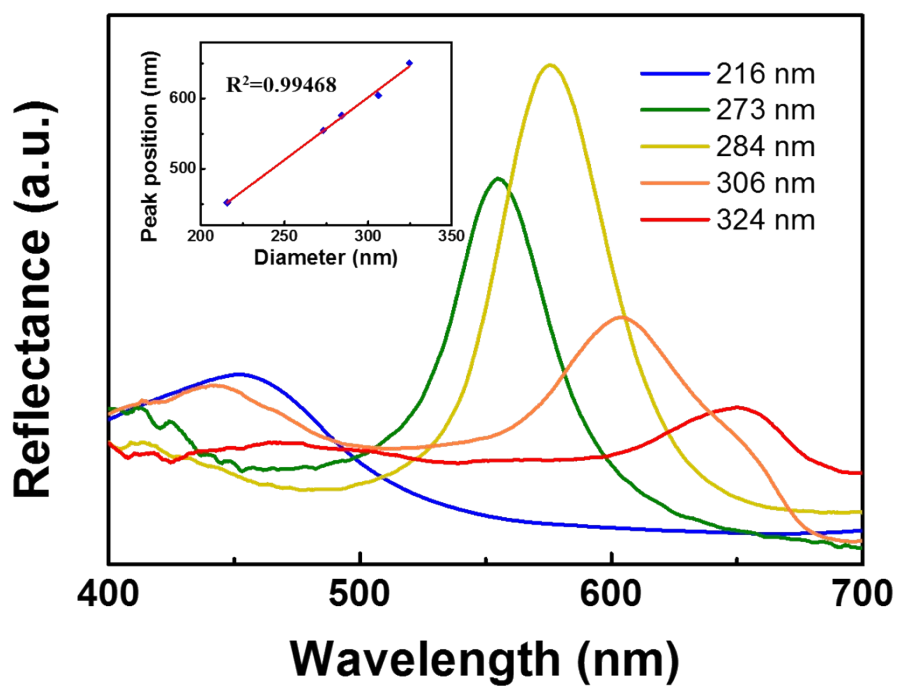


Figure S8. Reflection spectra of the MCFs containing PS/PMMA/PEA core-shell microspheres with different diameters (inset, experimental correlation between the peak position and microsphere diameter).

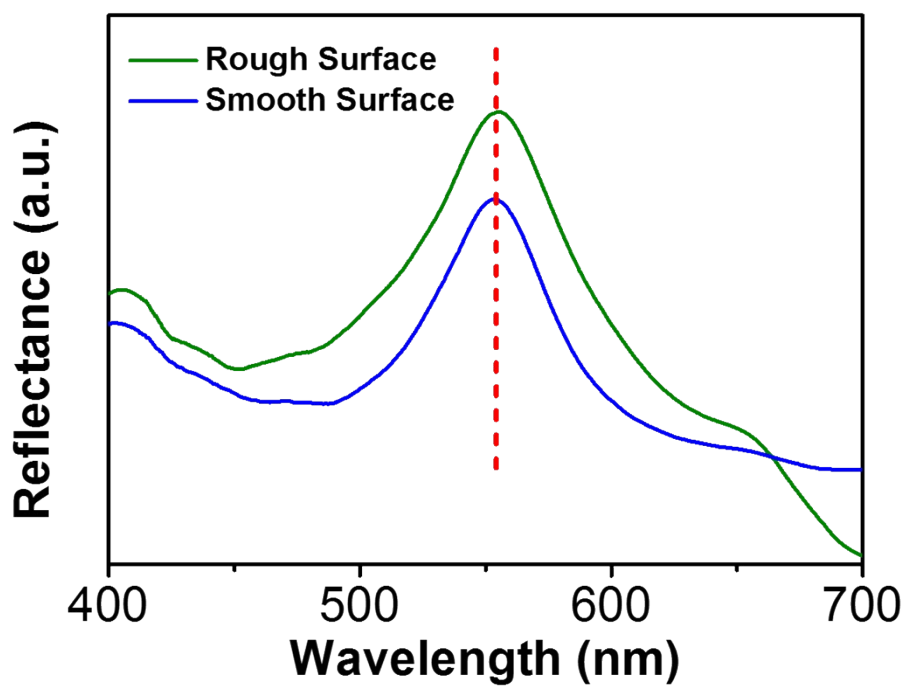


Figure S9. Reflection spectra of MCFs from multi-ply fibers with the rough surface and single-ply fiber with smooth surface.

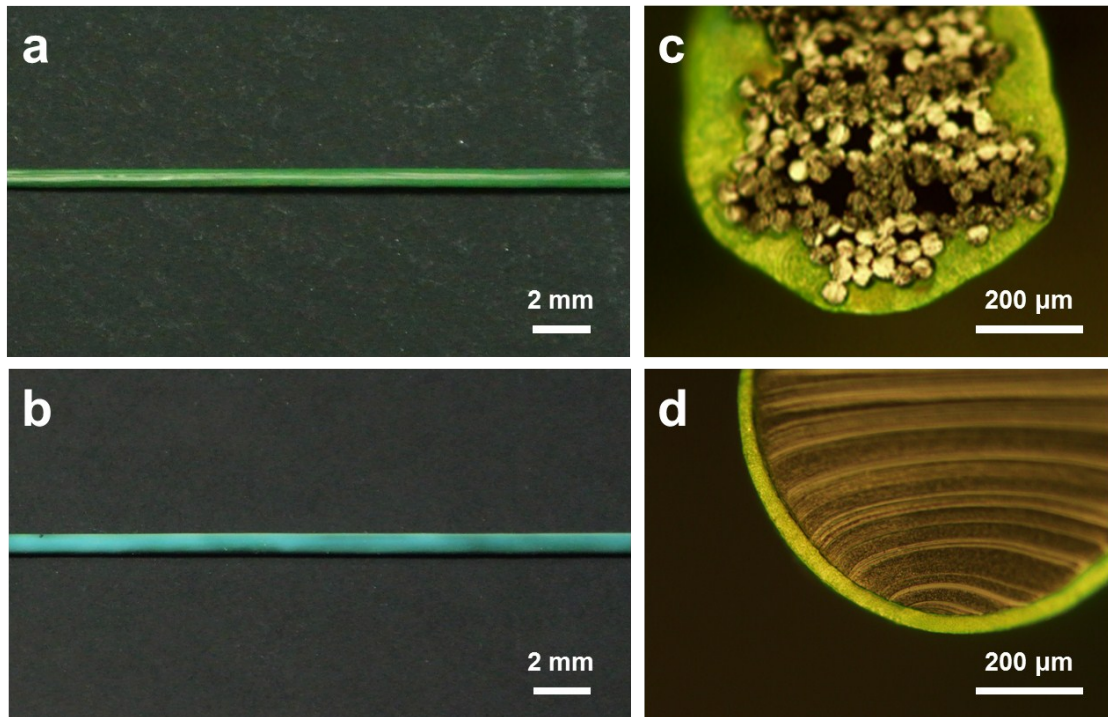


Figure S10. (a) and (b) Photographs of MCFs based on the multi-ply and single-ply fiber, respectively. (c) and (d) Cross-sectional optical micrographs of MCFs based on the multi-ply fiber at (a) and single-ply fiber at (b), respectively.

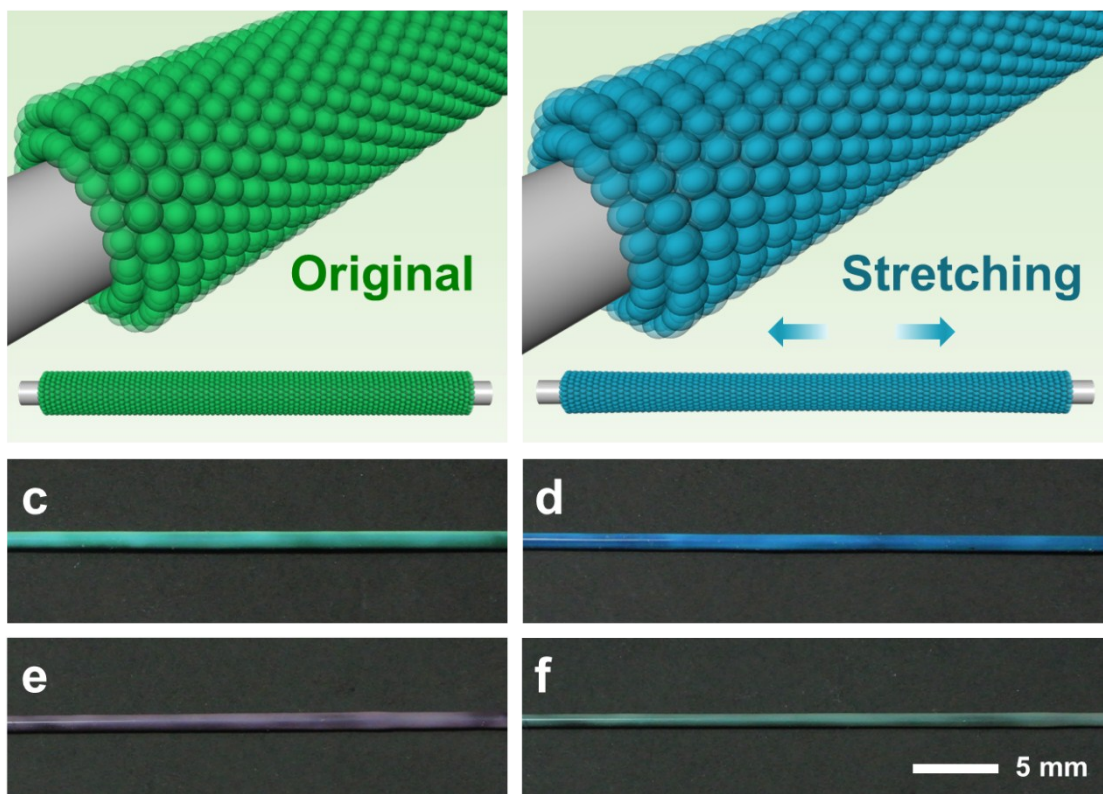


Figure S11. (a) and (b) Schematic illustrations to the mechanochromic behavior of the composite fiber before and after stretching, respectively. (c) and (d) Photographs of the fiber with colors of green and blue before and after stretching, respectively. (e) and (f) Photographs of the fiber with colors of red and green before and after stretching, respectively.

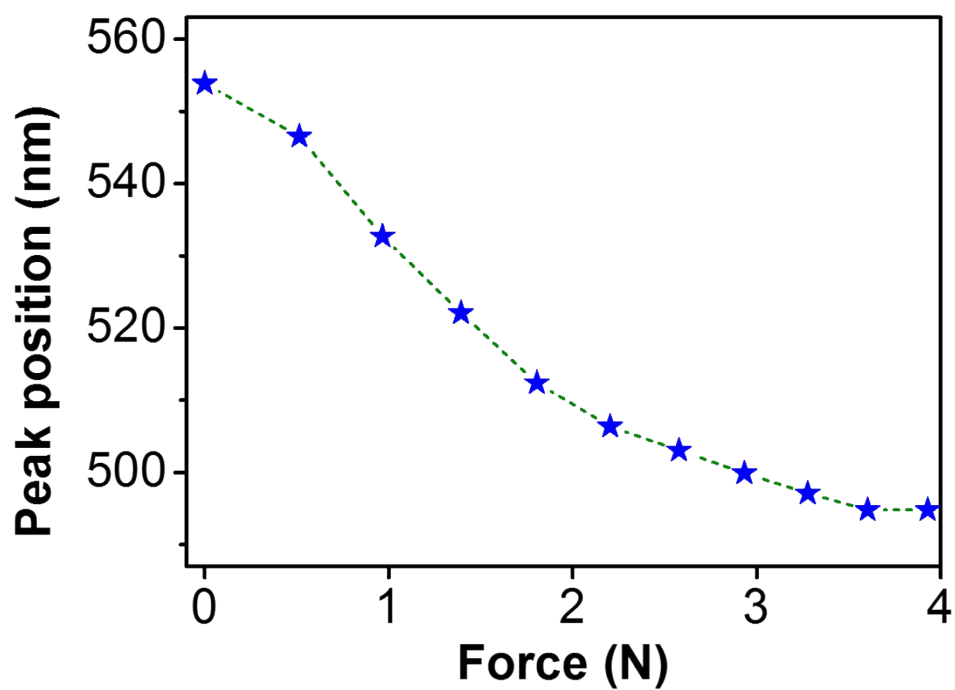


Figure S12. The variation of reflection peak position of MCFs with increasing forces.

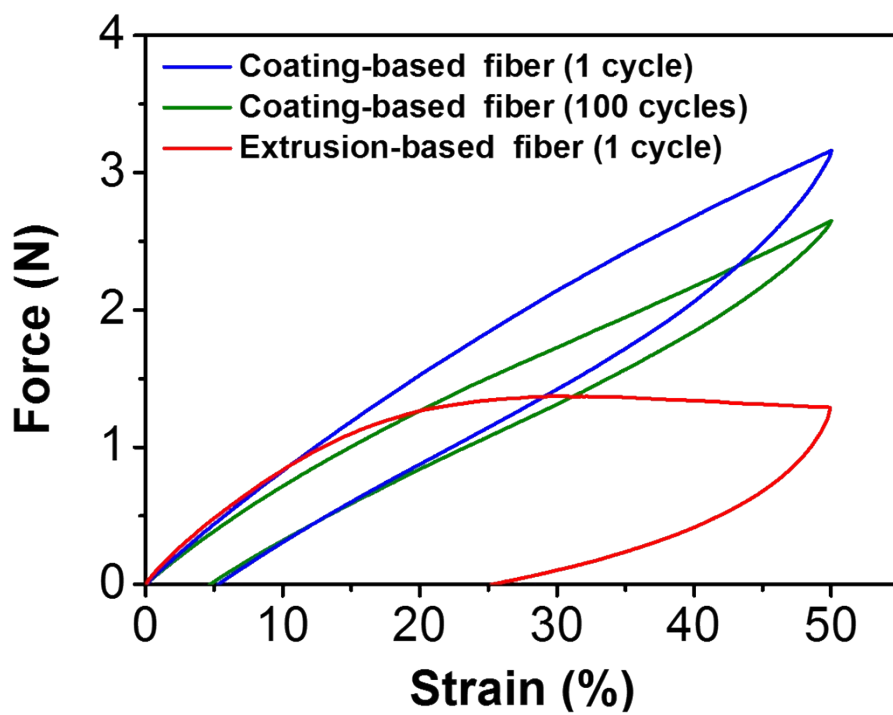


Figure S13. Stress-strain curves in the stretching and releasing cycles for coating-based and extrusion-based MCFs with a strain of 50%.

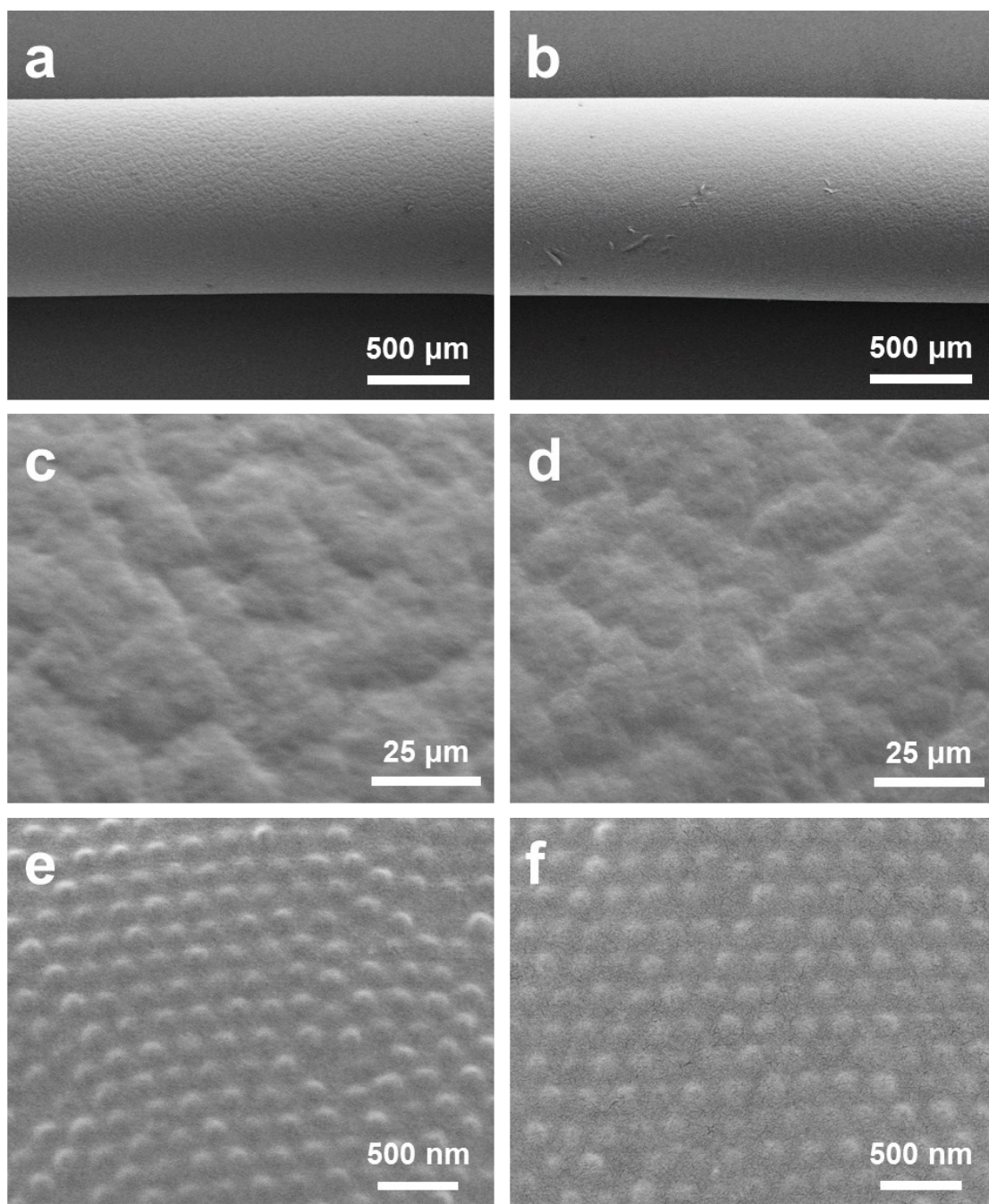


Figure S14. (a) and (b) SEM images of a MCFs before and after a standard laundry process in the washing machine. (c) and (e) Higher magnification of (a). (d) and (f) Higher magnification of (b).

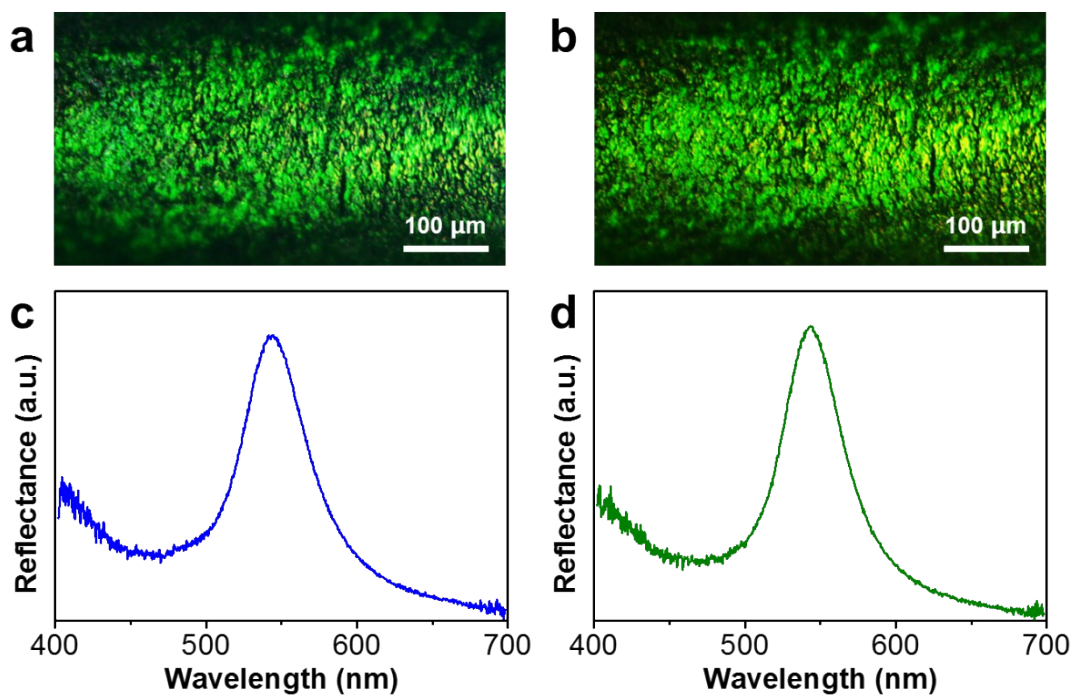


Figure S15. (a) and (b) Optical micrographs of MCF before and after a standard wash machine process, respectively. (c) and (d) Reflection spectra of fiber at (a) and (b), respectively.